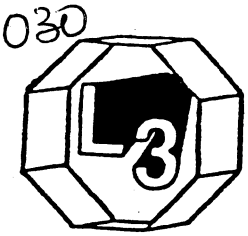

[redacted]

A Test of QCD based on 3-Jet Events from Z^0 Decays

The L3 Collaboration

ABSTRACT

We present a study of 43,000 3-jet events from Z^0 boson decays. Both the measured jet energy distributions and the event orientation are reproduced by second order QCD. An alternative model with scalar gluons fails to describe the data.

L3 Preprint #30
May 6, 1991

Introduction

Quarks and gluons of high momentum produced in e^+e^- annihilation form jets, which preserve the energy and the direction of the primary partons. The Z^0 resonance is ideal for a test of Quantum Chromodynamics (QCD) [1] for the following reasons: (a) Hadronization effects are small at such a center of mass energy. Jets are more collimated than those at lower energies. (b) The hadronic cross section is large. (c) Initial state hard photon radiation is strongly suppressed.

There is only one free parameter in QCD, which can be chosen as the strong coupling constant α_s at the scale $\mu = M_Z$. We have determined α_s from the fraction of 3-jet events and also from energy energy correlations at the Z^0 resonance [2, 3]. With this parameter known, all QCD matrix element calculations can be tested by comparing the measured jet distributions in multi-jet events to the theory.

Previously we have studied angular correlations in 4-jet events produced at the Z^0 resonance [4] and the fraction of 3-jet events as function of a jet resolution parameter [2]. In both these cases the measured distributions are reproduced by second order QCD calculations.

Here we present a study of 43,000 3-jet events observed at $\sqrt{s} = 91.2$ GeV in the L3 detector at LEP. We measure

(a) the jet energy distributions, and

(b) the orientation of the jets with respect to the beam direction.

The data are compared to second order QCD calculations and also to an alternative scalar gluon model.

Theoretical Basis

For unpolarized beams, an event of type $e^+e^- \rightarrow$ 3 jets can be described by four independent kinematical variables (apart from the jet masses):

x_1 = energy of the first jet normalized to the beam energy

x_2 = energy of the second jet normalized to the beam energy

θ = polar angle of the first jet with respect to the e^- direction

χ = angle between the jet plane and a plane spanned by the first jet and the beam

Here we do not distinguish between quark, antiquark and gluon jets. We refer to the most energetic jet as the 'first jet', i.e.: $x_1 > x_2 > x_3$ and $x_1 + x_2 + x_3 = 2$. Figures 1a and 1b illustrate those definitions.

The differential cross section for the process $e^+e^- \rightarrow$ 3 jets can be written in the general form

$$\frac{d\sigma}{dx_1\, dx_2\, d\cos\theta\, d\chi} = \sum_{i=1}^{4} f^i(\cos\theta, \chi) \cdot \frac{d\sigma^i}{dx_1\, dx_2} \qquad (1)$$

where the sum extends over four different Z^0 spin states and interference terms i [5].

While the functions f^i are determined by the initial state (e^+e^-) and the exchanged boson (Z^0), the helicity cross sections $d\sigma^i / dx_1\, dx_2$ are sensitive to the final state strong interactions ($q\bar{q}g$) and depend on the gluon spin (0 or 1). In lowest order, their form does not depend on the strong coupling constant, which appears as an overall factor. The helicity cross sections have been evaluated first for massless partons and photon exchange to $O(\alpha_s)$ in ref. [6] for vector gluons (QCD) and in ref. [7] for scalar gluons. Later the calculations have been refined by including mass effects [8], Z^0 exchange [5], and $O(\alpha_s^2)$ corrections [9] (for the spin-1 case).

The scalar gluon model is not compatible with various other measurements, in particular the energy dependence of jet rates [2]. Its purpose in this context is to provide a consistent theoretical alternative to QCD to show the sensitivity of the measured distributions.

Integrating (1) over the angular variables gives

$$\frac{d\sigma}{dx_1\, dx_2} = \frac{d\sigma^{\mathrm{U}}}{dx_1\, dx_2} + \frac{d\sigma^{\mathrm{L}}}{dx_1\, dx_2} \tag{2}$$

Here only the terms corresponding to transverse unpolarized Z^0 bosons (σ^{U}) and longitudinally polarized Z^0's (σ^{L}) contribute. This distribution and also the integrals of equation (2) over x_1 or x_2 are quite different for vector and scalar gluons and thus allow to discriminate between these models. The difference is mainly due to the poles at $x_1 = 1$ and $x_2 = 1$, which exist in QCD but not in the scalar gluon model. Also the Ellis-Karliner angle λ between the third and first jet, defined in the center of mass system of jets 2 and 3, allows a clear distinction between spin-1 and spin-0 gluons [10]. For massless partons [11]:

$$|\cos\lambda| = \frac{x_2 - x_3}{x_1}$$

The differential angular cross section can be calculated by integrating over a certain kinematic range of the variables x_1 and x_2. We choose to define it by the scaled invariant mass y of jets 2 and 3. For three massless partons $y = 1 - x_1$. Then

$$\frac{d\sigma}{d\cos\theta\, d\chi} = \sum_i f^i(\cos\theta, \chi) \cdot \sigma^i(y) \tag{3}$$

and, with the explicit expressions for f^i [5]:

$$\frac{d\sigma}{d\cos\theta} \propto 1 + \alpha(y) \cdot \cos^2\theta \tag{4}$$

$$\frac{d\sigma}{d\chi} \propto 1 + \beta(y) \cdot \cos(2\chi) \tag{5}$$

All distributions (3) - (5) depend on the gluon spin, and also the distribution

$$\frac{d\sigma}{d\cos\omega} \propto 1 + \gamma(y) \cdot \cos^2\omega \tag{6}$$

where ω is the angle of the normal to the 3-jet plane with respect to the beam direction:

$$\cos\omega = \sin\theta \cdot \sin\chi$$

The parameters α, β, γ are given by

$$\begin{aligned} \alpha &= \frac{\sigma^{U} - 2\sigma^{L}}{\sigma^{U} + 2\sigma^{L}} \\ \beta &= \frac{\sigma^{T}}{\sigma^{U} + \sigma^{L}} \\ \gamma &= -1/3 \cdot \frac{\sigma^{U} - 2\sigma^{L} + 6\sigma^{T}}{\sigma^{U} + 2/3\,\sigma^{L} + 2/3\,\sigma^{T}} \end{aligned}$$

For the well-known case of 2-jet events the parameter α is equal to 1. In first order QCD the helicity cross section corresponding to the interference between helicity +1 and helicity -1 states of the Z^0 is $\sigma^{T} = \frac{1}{2}\sigma^{L}$ and therefore $\gamma = -1/3$.

In the vector gluon case the cross sections σ^{U}, σ^{L} and σ^{T} for $e^+e^- \to \gamma \to q\bar{q}g$ and for $e^+e^- \to Z^0 \to q\bar{q}g$ are identical. For spin-0 gluons the helicity cross section terms proportional to v_q^2 and a_q^2 are different from each other. Here v_q and a_q denote the vector and axial vector couplings of the quark q to the Z^0 boson, respectively. Thus in the scalar gluon case the 3-jet distributions for Z^0 exchange differ from those for γ exchange.

In this paper we compare the measured 2-dimensional distributions (2) ('Dalitz plot') and (3), and the 1-dim. distributions in the variables x_2, x_3, $\cos\lambda$, $\cos\theta$, χ and $\cos\omega$ to the theoretical predictions by QCD and by the scalar gluon model. We also investigate the dependence of the mean values $\langle x_2\rangle$, $\langle x_3\rangle$, $\langle\cos\lambda\rangle$, and the parameters α, β and γ, on the scaled invariant mass y.

The L3 Detector

The L3 detector covers 99% of 4π [12]. The detector consists of a central tracking chamber, a high resolution electromagnetic calorimeter composed of bismuth germanium oxide crystals, a ring of scintillation counters, a uranium and brass hadron calorimeter with proportional wire chamber readout, and an accurate muon chamber system. These detectors are installed in a 12 m diameter magnet which provides a uniform field of 0.5 T along the beam direction.

For the present analysis, we use the data collected in the following ranges of polar angles:

- for the electromagnetic calorimeter, $42° < \theta < 138°$,
- for the hadron calorimeter, $5° < \theta < 175°$.

The fine segmentation of these detectors allow us to measure the axis of jets with an angular resolution of approximately 2.5°, and to measure the total energy of hadronic events from Z^0 decay with a resolution of about 10% [13].

Selection of Hadronic Events

Events collected at the pole of the Z^0 resonance ($\sqrt{s} = 91.2$ GeV) from the 1990 LEP running period are used for this analysis.

The primary trigger for hadronic events requires a total energy of about 15 GeV in the calorimeters. This trigger is in logical OR with a trigger using the barrel scintillation counters and with a charged track trigger. The combined trigger efficiency for selected hadronic events exceeds 99.5%.

The selection of $e^+e^- \rightarrow$ *hadrons* events is based on the energy measured in the electromagnetic detector and in the hadron calorimeter. Events are accepted if

$$0.6 < \frac{E_{\rm vis}}{\sqrt{s}} < 1.4$$

$$\frac{|E_{\parallel}|}{E_{\rm vis}} < 0.40, \; \frac{E_{\perp}}{E_{\rm vis}} < 0.40$$

$$N_{cluster} \geq 12$$

where $E_{\rm vis}$ is the total energy observed in the detector, $E_{\parallel}$ is the energy imbalance along the beam direction, and $E_{\perp}$ is the transverse energy imbalance. An algorithm was used to group neighbouring calorimeter hits, which are probably produced by the same particle, into clusters. Only clusters with a total energy above 100 MeV were used. The algorithm normally reconstructs one cluster for each particle produced near the interaction point. Thus the cut on the number of clusters rejects low multiplicity events (e^+e^-, $\mu^+\mu^-$, $\tau^+\tau^-$).

In total 82,300 events were selected.

Applying the same cuts to simulated events, we find that 97% of the hadronic decays from the Z^0 are accepted. The contamination from final states e^+e^-, $\tau^+\tau^-$ and hadronic production via two photon processes in the event sample is below 0.2% and can be neglected.

Monte Carlo events were generated by the parton shower programs JETSET 7.2 [14] and HERWIG 4.3 [15] with values for the QCD scale and fragmentation parameters as determined from a fit to our data [3, 16]. The generated events were passed through the L3 detector simulation [17] which includes the effects of energy loss, multiple scattering, interactions and decays in the detector materials and beam pipe.

Analysis of 3-Jet Events

Jets are reconstructed out of clusters in the calorimeters. We have investigated several jet algorithms to optimize the angular resolution of the jets. The best method starts with the 'JADE' version [18] of an invariant mass algorithm. In this recombination scheme, there is a close agreement between jet rates at parton and detector level. The jet angular resolution is improved by (a) adding up the four momenta of the clusters within a cone

of half opening angle of 30° around the initial jet directions, (b) redefining the jets as the sums of four momenta, and (c) iterating the procedure until it converges. The initial jet directions are those given by the JADE algorithm. As a cross check to this method, we also use a different jet algorithm, with only angular criteria on energy ordered clusters for recombination, as used by CELLO [19]. The second method gives a comparable jet angular resolution, but is inferior in determining the correct jet multiplicity.

A jet resolution parameter $y_{\rm cut} \geq 0.02$ corresponding to a jet pair mass of 13 GeV or more is used to select 3-jet events for this analysis. We divide the event sample into six subsamples according to the jet resolution parameter $y_{\rm cut}$: 0.02-0.05, 0.05-0.10, 0.10-0.15, 0.15-0.20, 0.20-0.25 and > 0.25. The corresponding numbers of events are 20800, 13100, 5200, 2500, 1200 and 550, respectively. An event is included only, if it is a 3-jet event for both the lower and upper $y_{\rm cut}$ values defining the $y_{\rm cut}$ region considered.

All the kinematic quantities studied here, are computed using the measured jet directions. The formulae are strictly correct only for massless partons. The Dalitz plot variable, x_i, can be determined using [11]

$$x_i = \frac{2 \sin \psi_i}{\sin \psi_1 + \sin \psi_2 + \sin \psi_3}$$

where ψ_i is the angle between the two jets different from jet i (see fig. 1a). The use of this formula is justified since the measured 3-jet events are planar to a good approximation: for 95% of the events the sum of the three angles, $\psi_1 + \psi_2 + \psi_3$, exceeds $0.98 \cdot 2\pi$. The Ellis-Karliner λ angle is then given by

$$|\cos \lambda| = \frac{\sin \psi_2 - \sin \psi_3}{\sin \psi_1}$$

The angles χ and ω have been reconstructed using the two most energetic jets to define the event plane.

The detector resolution has been studied using Monte Carlo events generated by the parton shower program JETSET 7.2, as described in the previous section. Table 1 summarizes the detector resolution for the Dalitz plot and orientation variables. We have chosen bin widths typically twice the size of the resolution so that bin-to-bin migration is small.

variable	detector resol.	hadronization
x_2	0.04	0.04
x_3	0.05	0.04
$\cos \lambda$	0.09	0.08
$\cos \theta$	0.02	0.01
χ	9°	6°
$\cos \omega$	0.05	0.03

Table 1: Experimental resolution and hadronization effects (Half Width Half Maximum) for the quantities x_2, x_3, $\cos \lambda$, $\cos \theta$, χ and $\cos \omega$ averaged over the entire event sample.

We find that the observed distributions can be described by the JETSET 7.2 Monte Carlo with detector simulation. The measured distributions are corrected for detector

resolution on a bin-by-bin basis. Some 3-jet events at generator level migrate to a different category at detector level, while non-3-jet events at generator level can become 3-jet events at detector level. From a Monte-Carlo study both effects are found to be small ($\sim$ 5%) and have been corrected for again on a bin-by-bin basis. The observed distributions are also corrected for acceptance and shown in figures 2 and 3. The overall correction factor for each bin equals 1 within typically 10%.

The uncertainties in the detector correction are studied (a) by changing the energy response in different detector components in the Monte Carlo simulation by up to 10%, (b) by using the HERWIG 4.3 [15] parton shower Monte Carlo program (instead of JETSET 7.2) with detector simulation to correct the data, and (c) by using different methods of background subtractions. We find a total systematic uncertainty in the correction factors of 5%. This error has been added in quadrature to the statistical error as shown in figures 2 and 3.

Table 2 and figure 4 show the mean values of the variables x_2, x_3 and $\cos\lambda$ for the six $y_{\rm cut}$ intervals. The errors include statistical errors and systematic uncertainties in the detector correction. The systematic error in the mean is estimated by using several sets of corrected distributions, corresponding to different energy response functions, different Monte Carlo models, and different background correction methods.

$y_{\rm cut}$	$\langle x_2 \rangle$	$\langle x_3 \rangle$	$\langle \cos\lambda \rangle$
0.02-0.05	0.845 ± 0.003	0.181 ± 0.006	0.681 ± 0.010
0.05-0.10	0.811 ± 0.003	0.249 ± 0.006	0.596 ± 0.010
0.10-0.15	0.778 ± 0.003	0.330 ± 0.006	0.500 ± 0.010
0.15-0.20	0.738 ± 0.003	0.421 ± 0.006	0.373 ± 0.010
0.20-0.25	0.708 ± 0.004	0.500 ± 0.007	0.263 ± 0.011
> 0.25	0.678 ± 0.004	0.574 ± 0.007	0.142 ± 0.011

Table 2: Measured mean values of the variables x_2, x_3, $\cos\lambda$ as a function of $y_{\rm cut}$, corrected for detector effects. The errors include statistical and systematic uncertainties.

We fit the equations (4)-(6) to the angular distributions to obtain the parameters α, β and γ. In all cases the χ^2 values of the fits are close to the number of degrees of freedom. The values of α, β and γ are shown in table 3 and figure 5 as a function of $y_{\rm cut}$. We estimate the systematic errors in these parameters in a way similar to the one described above for the mean values.

$y_{\rm cut}$	α	β	γ
0.02-0.05	0.85 ± 0.16	0.05 ± 0.03	-0.35 ± 0.06
0.05-0.10	0.79 ± 0.16	0.01 ± 0.03	-0.29 ± 0.07
0.10-0.15	0.88 ± 0.18	0.00 ± 0.04	-0.29 ± 0.07
0.15-0.20	1.02 ± 0.21	0.01 ± 0.05	-0.34 ± 0.08
0.20-0.25	0.74 ± 0.23	0.00 ± 0.06	-0.24 ± 0.11
> 0.25	0.60 ± 0.30	-0.01 ± 0.08	-0.19 ± 0.16

Table 3: parameters α, β and γ as a function of $y_{\rm cut}$, corrected for detector effects. The errors include statistical and systematic uncertainties.

For low values of y_{cut} the errors in tables 2,3 are dominated by systematic uncertainties.

Theoretical Models

To compute the QCD predictions we use the matrix element option in JETSET 7.2 which is based on the calculations given in ref. [20] and includes terms up to $O(\alpha_s^2)$ for the jet energy distributions. We applied the approximate $O(\alpha_s^2)$ correction [9] to the jet plane orientation, which is available only to $O(\alpha_s^1)$ in the original program version. We used a value of $\Lambda_{\overline{MS}}$ as measured from the 3-jet rate [2] and a renormalization scale $\mu^2 = 0.08 \cdot s$. The distributions calculated to second order in α_s deviate only little from those obtained in first order; the biggest effect is seen in the parameter α in equation (4), which is increased by up to 0.05; this change is small compared to the experimental error.

To simulate the hadronization process we again use the matrix element option in JETSET 7.2 with fragmentation parameters as determined from a comparison of predicted and measured distributions for several event shape variables. The effect of hadronization is small. Table 1 shows the effect of hadronization for the principal quantities used in this analysis. The mean values $\langle x_2 \rangle$, $\langle x_3 \rangle$, $\langle \cos\lambda \rangle$ and also the parameters α, β and γ are modified by less than 0.02 when going from the parton to the hadron level. The shape of the angular distributions remains unchanged.

In addition we include initial and final state radiation, which has a negligible effect on the quantities investigated here.

For the computation of the scalar gluon distributions we use the generator JETSET 7.2 with modified helicity cross sections which include both vector and axial vector contributions as appropriate for Z^0 boson exchange [5]. The $O(\alpha_s^1)$ parton distributions are then corrected (bin-by-bin) using correction factors f determined for the vector-gluon case: $f = \mathrm{MC}^{(2)}_{\mathrm{hadron}}/\mathrm{MC}^{(1)}_{\mathrm{parton}}$. The numerator is calculated with the second order QCD matrix element generator plus fragmentation and photon radiation. $\mathrm{MC}^{(1)}_{\mathrm{parton}}$ is obtained using the first order generator at the parton level. This procedure is applied since the contribution of 4-parton final states is not known in the scalar gluon case, and since fragmentation is not well defined in this model. Typically f is in the range 0.9–1.1 for the Dalitz plot variables and in the range 0.97-1.03 for the $\cos\theta$, χ and $\cos\omega$ distributions.

To study theoretical uncertainties we vary the renormalization scale and the fragmentation parameters. A change in the scale in the range $0.002 \cdot s \leq \mu^2 \leq s$ and a corresponding change in $\Lambda_{\overline{MS}}$ [2] modifies the mean values of the variables x_2, x_3 and $\cos\lambda$ by less than 0.01. The variation in the parameters α, β and γ is of the order 0.02. The sensitivity to a change in the fragmentation parameters, in a range compatible with our measured event shape distributions, is similar to that for the scale variation. When calculating χ^2 values we assign a 5% relative error per bin for the Dalitz plot variables and an uncertainty of 3% for the angular variables $\cos\theta$, χ and $\cos\omega$.

Statistical uncertainties due to limited Monte Carlo generator statistics can be neglected, since we generated event samples exceeding the size of the data event sample by more than a factor of 10.

Results and Comparison to Theoretical Models

We compare the measured two-dimensional distributions in the variables x_2, x_3 (equation (2)) and $\cos\theta$, χ (equation (3)) to the predictions of the vector and scalar models, normalized to the number of data events. Here all 3-jet events have been used. The resulting χ^2 values and corresponding probabilities are given in table 4. Each of the two-dimensional distributions can be reproduced by QCD while the scalar gluon model predictions fail to describe either of them.

	vector gluons		scalar gluons	
2-dim. distr.	χ^2/NDF	probab.	χ^2/NDF	probab.
x_2, x_3	37/36	0.42	2145/37	$< 10^{-10}$
$\cos\theta$, χ	113/99	0.16	150/99	$7 \cdot 10^{-4}$

Table 4: Results of a comparison of measured two-dimensional distributions in the variables x_2, x_3 and $\cos\theta$, χ to the predictions of the vector and scalar gluon models. Given are the χ^2 value, the corresponding number of degrees of freedom and the probability. For the comparison of the Dalitz plots only those bins have been considered in which there are at least 0.1% of the total number of events.

Figures 2 and 3 compare the measured one-dimensional distributions in the variables x_2, x_3, $\cos\lambda$, $\cos\theta$, χ and $\cos\omega$ with predicted ones for the lowest and highest $y_{\rm cut}$ regions, $0.02 \leq y_{\rm cut} < 0.05$ and $y_{\rm cut} > 0.25$. Again the theoretical curves are normalized to the number of data events. In all cases good agreement is found between the QCD predictions and the measurements. The scalar model fails to describe the data, which can be seen best in figure 2 for the Dalitz plot variables. The data points in figure 2a exhibit a strong rise for $x_2 \to 1$ as expected from the pole in QCD, but not predicted in the scalar gluon model. The decrease of the mean value of the x_2 distribution with increasing $y_{\rm cut}$ is due to the relation $x_2 < x_1 \approx 1 - y_{\rm cut}$. The mean value $\langle x_3 \rangle$ increases with $y_{\rm cut}$ since $x_3 = 2 - x_1 - x_2$.

To study the dependence on the jet resolution parameter $y_{\rm cut}$ we have computed the mean values of the variables x_2, x_3 and $\cos\lambda$ for the six $y_{\rm cut}$ regions defined above. They are shown in table 2 and in figure 4 together with the model predictions as a function of the jet resolution parameter $y_{\rm cut}$. Similarly we show in table 3 and figure 5 the $y_{\rm cut}$ dependence of the fitted parameters α, β and γ. Again, only QCD can reproduce the measurements.

The comparison between data and theory using the alternative jet algorithm gives results comparable to those described above.

Comparison to Previous Measurements

Measurements of the Dalitz plot variables and of the Ellis-Karliner angle, and comparisons to first-order QCD and the scalar gluon model, have been published previously [11, 21, 19, 22]. These analyses were based on relatively small event samples (100—2000

3-jet events) obtained at center of mass energies around 30 GeV, where hadronic final states are produced dominantly via γ exchange. Due to large fragmentation effects for low energy jets only events corresponding to $y_{\rm cut} \geq 0.07 - 0.10$ could be used. As a consequence the pole structure in the distribution of the variables x_1 and x_2, which is predicted for vector gluons only, can not be seen very well. In all previous studies the first order QCD predictions were found to agree with the measurements, while the scalar gluon model could not reproduce the data.

Also the orientation of 3-jet events has been studied using about 2000 events corresponding to $y_{\rm cut} \geq 0.15$ at $\sqrt{s} \approx 30$ GeV [23]. QCD to first order reproduces the measured distributions; a comparison to the scalar gluon model has not been made.

Summary and Conclusions

We present the first study of the jet energy distributions and the event orientation for a large sample of 3-jet events at $\sqrt{s} = 91.2$ GeV. The measured distributions and also their dependence on the invariant mass of the two least energetic jets are reproduced by second order QCD. An alternative scalar gluon model fails to describe the data.

Acknowledgments

We wish to express our gratitude to the CERN accelerator divisions for the excellent performance of the LEP machine. We acknowledge the effort of all engineers and technicians who have participated in the construction and maintenance of this experiment. We thank T. Sjöstrand and P. Zerwas for helpful discussions.

The L3 Collaboration:

B.Adeva[15] O.Adriani[13] M.Aguilar-Benitez[23] H.Akbari[5] J.Alcaraz[23] A.Aloisio[25] G.Alverson[9] M.G.Alviggi[25] Q.An[16] H.Anderhub[40] A.L.Anderson[12] V.P.Andreev[14] T.Angelov[12] L.Antonov[35] D.Antreasyan[7] P.Arce[23] A.Arefiev[24] T.Azemoon[3] T.Aziz[8] P.V.K.S.Baba[16] P.Bagnaia[31] J.A.Bakken[30] L.Baksay[36] R.C.Ball[3] S.Banerjee[8] J.Bao[5] R.Barillère[15] L.Barone[31] A.Bay[17] U.Becker[12] F.Behner[40] J.Behrens[40] S.Beingessner[4] Gy.L.Bencze[10,15] J.Berdugo[23] P.Berges[12] B.Bertucci[31] B.L.Betev[35] A.Biland[40] R.Bizzarri[31] J.J.Blaising[4] P.Blömeke[1] B.Blumenfeld[5] G.J.Bobbink[2] M.Bocciolini[13] R.Bock[1] A.Böhm[1,15] B.Borgia[31] D.Bourilkov[35] M.Bourquin[17] D.Boutigny[4] B.Bouwens[2] J.G.Branson[32] I.C.Brock[29] F.Bruyant[15] C.Buisson[22] A.Bujak[37] J.D.Burger[12] J.P.Burq[22] J.Busenitz[36] X.D.Cai[16] M.Capell[20] F.Carbonara[25] P.Cardenal[15] F.Carminati[13] A.M.Cartacci[13] M.Cerrada[23] F.Cesaroni[31] Y.H.Chang[12] U.K.Chaturvedi[16] M.Chemarin[22] A.Chen[42] C.Chen[6] G.M.Chen[6] H.F.Chen[18] H.S.Chen[6] M.Chen[12] M.L.Chen[3] W.Y.Chen[16] G.Chiefari[25] C.Y.Chien[5] F.Chollet[4] C.Civinini[13] I.Clare[12] R.Clare[12] H.O.Cohn[27] G.Coignet[4] N.Colino[15] V.Commichau[1] G.Conforto[13] A.Contin[15] F.Crijns[26] X.Y.Cui[16] T.S.Dai[12] R.D'Alessandro[13] R.de Asmundis[25] A.Degré[15,4] K.Deiters[12] E.Dénes[10,15] P.Denes[30] F.DeNotaristefani[31] M.Dhina[40] D.DiBitonto[36] M.Diemoz[31] H.R.Dimitrov[35] C.Dionisi[31] M.T.Dova[16] E.Drago[25] T.Driever[26] D.Duchesneau[17] P.Duinker[2] I.Duran[23] H.El Mamouni[22] A.Engler[29] F.J.Eppling[12] F.C.Erné[2] P.Extermann[17] R.Fabbretti[38] M.Fabre[40] S.Falciano[31] Q.Fan[16] S.J.Fan[34] O.Fackler[20] J.Fay[22] T.Ferguson[29] G.Fernandez[23] F.Ferroni[31,15] H.Fesefeldt[1] J.Field[17] F.Filthaut[26] G.Finocchiaro[31] P.H.Fisher[5] G.Forconi[17] T.Foreman[2] K.Freudenreich[40] W.Friebel[39] M.Fukushima[12] M.Gailloud[19] Yu.Galaktionov[24] E.Gallo[13] S.N.Ganguli[8] P.Garcia-Abia[23] S.S.Gau[42] D.Gele[22] S.Gentile[31] M.Glaubman[9] S.Goldfarb[3] Z.F.Gong[18] E.Gonzalez[23] A.Gordeev[24] P.Göttlicher[1] D.Goujon[17] G.Gratta[28] C.Grinnell[12] M.Gruenewald[28] M.Guanziroli[16] J.K.Guo[34] A.Gurtu[8] H.R.Gustafson[3] L.J.Gutay[37] H.Haan[1] A.Hasan[16] D.Hauschildt[2] C.F.He[34] T.Hebbeker[1] M.Hebert[32] G.Herten[12] U.Herten[1] A.Hervé[15] K.Hilgers[1] H.Hofer[40] H.Hoorani[16] L.S.Hsu[42] G.Hu[16] G.Q.Hu[34] B.Ille[22] M.M.Ilyas[16] V.Innocente[25,15] E.Isiksal[40] H.Janssen[15] B.N.Jin[6] L.W.Jones[3] A.Kasser[19] R.A.Khan[16] Yu.Kamyshkov[24,27] Y.Karyotakis[4,15] M.Kaur[16] S.Khokhar[16] V.Khoze[14] M.N.Kienzle-Focacci[17] W.Kinnison[21] D.Kirkby[28] W.Kittel[26] A.Klimentov[24] A.C.König[26] O.Kornadt[1] V.Koutsenko[24,12] R.W.Kraemer[29] T.Kramer[12] V.R.Krastev[35] W.Krenz[1] J.Krizmanic[5] K.S.Kumar[11] V.Kumar[16] A.Kunin[11,24] V.Lalieu[17] G.Landi[13] K.Lanius[15] D.Lanske[1] S.Lanzano[25] P.Lebrun[22] P.Lecomte[40] P.Lecoq[15] P.Le Coultre[40] D.Lee[21] I.Leedom[9] J.M.Le Goff[15] L.Leistam[15] R.Leiste[39] M.Lenti[13] E.Leonardi[31] J.Lettry[40] P.M.Levchenko[14] X.Leytens[2] C.Li[18,16] H.T.Li[6] J.F.Li[16] L.Li[38] P.J.Li[34] Q.Li[16] X.G.Li[6] J.Y.Liao[34] Z.Y.Lin[18] F.L.Linde[29] B.Lindemann[1] D.Linnhofer[40] R.Liu[16] Y.Liu[16] W.Lohmann[39] E.Longo[31] Y.S.Lu[6] J.M.Lubbers[15] K.Lübelsmeyer[1] C.Luci[15] D.Luckey[7,12] L.Ludovici[31] L.Luminari[31] W.G.Ma[18] M.MacDermott[40] R.Magahiz[33] M.Maire[4] P.K.Malhotra[8] R.Malik[16] A.Malinin[24] C.Maña[23] D.N.Mao[3] Y.F.Mao[6] M.Maolinbay[40] P.Marchesini[40] A.Marchionni[13] J.P.Martin[22] L.Martinez-Laso[15] F.Marzano[31] G.G.G.Massaro[2] T.Matsuda[12] K.Mazumdar[8] P.McBride[11] T.McMahon[37] D.McNally[40] Th.Meinholz[1] M.Merk[26] L.Merola[25] M.Meschini[13] W.J.Metzger[26] Y.Mi[16] G.B.Mills[21] Y.Mir[16] G.Mirabelli[31] J.Mnich[1] M.Möller[1] B.Monteleoni[13] G.Morand[17] R.Morand[4] S.Morganti[31] N.E.Moulai[16] R.Mount[28] S.Müller[1] E.Nagy[10] M.Napolitano[25] H.Newman[28] C.Neyer[40] M.A.Niaz[16] L.Niessen[1] H.Nowak[39] D.Pandoulas[1] F.Pauss[40] F.Plasil[27] G.Passaleva[13] G.Paternoster[25] S.Patricelli[25] Y.J.Pei[1] D.Perret-Gallix[4] J.Perrier[17] A.Pevsner[5] M.Pieri[13] P.A.Piroué[30] V.Plyaskin[24] M.Pohl[40] V.Pojidaev[24] N.Produit[17] J.M.Qian[3] K.N.Qureshi[16] R.Raghavan[8] G.Rahal-Callot[40] P.Razis[36] K.Read[27] D.Ren[40] Z.Ren[16] S.Reucroft[9] A.Ricker[1] S.Riemann[39] O.Rind[3] C.Rippich[29] H.A.Rizvi[16] B.P.Roe[3] M.Röhner[1] S.Röhner[1] L.Romero[23] J.Rose[1] S.Rosier-Lees[4] R.Rosmalen[26] Ph.Rosselet[19] A.Rubbia[12] J.A.Rubio[15,23] M.Rubio[15] W.Ruckstuhl[17] H.Rykaczewski[40] M.Sachwitz[39,15] J.Salicio[15,23] J.M.Salicio[23] G.Sanders[21] M.S.Sarakinos[12] G.Sartorelli[7,16] G.Sauvage[4] A.Savin[24] V.Schegelsky[14] K.Schmiemann[1] D.Schmitz[1] P.Schmitz[1] M.Schneegans[4] H.Schopper[41] D.J.Schotanus[26] S.Shotkin[12] H.J.Schreiber[39] R.Schulte[1] S.Schulte[1] K.Schultze[1] J.Schütte[11] J.Schwenke[1] G.Schwering[1] C.Sciacca[25] I.Scott[11] R.Sehgal[16] P.G.Seiler[38] J.C.Sens[2] I.Sheer[32] D.Z.Shen[34] V.Shevchenko[24] S.Shevchenko[24] X.R.Shi[29] K.Shmakov[24] V.Shoutko[24] E.Shumilov[24] N.Smirnov[14] E.Soderstrom[30] A.Sopczak[32] C.Spartiotis[5] T.Spickermann[1] P.Spillantini[13] R.Starosta[1] M.Steuer[7,12] D.P.Stickland[30] F.Sticozzi[12] W.Stoeffl[20] H.Stone[17] K.Strauch[11] B.C.Stringfellow[37] K.Sudhakar[8,1] G.Sultanov[16] R.L.Sumner[30] L.Z.Sun[18,16] H.Suter[40] R.B.Sutton[29] J.D.Swain[16] A.A.Syed[16] X.W.Tang[6] E.Tarkovsky[24] L.Taylor[9] C.Timmermans[26] Samuel C.C.Ting[12] S.M.Ting[12] Y.P.Tong[42] F.Tonisch[39] M.Tonutti[1] S.C.Tonwar[8] J.Tóth[10,15] G.Trowitzsch[39] C.Tully[28] K.L.Tung[6] J.Ulbricht[40] L.Urbán[10] U.Uwer[1] E.Valente[31] R.T.Van de Walle[26] I.Vetlitsky[24] G.Viertel[40] P.Vikas[16] U.Vikas[16] M.Vivargent[4,12] H.Vogel[29] H.Vogt[39] G.Von Dardel[15] I.Vorobiev[24] A.A.Vorobyov[14] An.A.Vorobyov[14] L.Vuilleumier[19] M.Wadhwa[16] W.Wallraff[1] C.R.Wang[18] G.H.Wang[29] J.H.Wang[6] Q.F.Wang[11] X.L.Wang[18] Y.F.Wang[13] Z.Wang[16] Z.M.Wang[16,18] A.Weber[1] J.Weber[40] R.Weill[19]

T.J.Wenaus,[20] J.Wenninger,[17] M.White,[12] C.Willmott,[23] F.Wittgenstein,[15] D.Wright,[30] R.J.Wu,[6] S.L.Wu,[16] S.X.Wu,[16] Y.G.Wu,[6] B.Wysłouch,[12] Y.Y.Xie,[34] Y.D.Xu,[6] Z.Z.Xu,[18] Z.L.Xue,[34] D.S.Yan,[34] X.J.Yan,[12] B.Z.Yang,[18] C.G.Yang,[6] G.Yang,[16] K.S.Yang,[6] Q.Y.Yang,[6] Z.Q.Yang,[34] C.H.Ye,[16] J.B.Ye,[40,18] Q.Ye,[16] S.C.Yeh,[42] Z.W.Yin,[34] J.M.You,[16] M.Yzerman,[2] C.Zaccardelli,[28] P.Zemp,[40] M.Zeng,[16] Y.Zeng,[1] D.H.Zhang,[2] Z.P.Zhang,[18,16] J.F.Zhou,[1] R.Y.Zhu,[28] H.L.Zhuang,[6] A.Zichichi.[15,16]

---

1 I. Physikalisches Institut, RWTH, Aachen, Federal Republic of Germany§
III. Physikalisches Institut, RWTH, Aachen, Federal Republic of Germany§
2 National Institute for High Energy Physics, NIKHEF, Amsterdam, The Netherlands
3 University of Michigan, Ann Arbor, Michigan, United States of America
4 Laboratoire de Physique des Particules, LAPP, Annecy, France
5 Johns Hopkins University, Baltimore, Maryland, United States of America
6 Institute of High Energy Physics, IHEP, Beijing, China
7 INFN-Sezione di Bologna, Italy
8 Tata Institute of Fundamental Research, Bombay, India
9 Northeastern University, Boston, Massachusetts, United States of America
10 Central Research Institute for Physics of the Hungarian Academy of Sciences, Budapest, Hungary
11 Harvard University, Cambridge, Massachusetts, United States of America
12 Massachusetts Institute of Technology, Cambridge, Massachusetts, United States of America
13 INFN Sezione di Firenze and University of Firenze, Italy
14 Leningrad Nuclear Physics Institute, Gatchina, Soviet Union
15 European Laboratory for Particle Physics, CERN, Geneva, Switzerland
16 World Laboratory, FBLJA Project, Geneva, Switzerland
17 University of Geneva, Geneva, Switzerland
18 University of Science and Technology of China, Hefei, China
19 University of Lausanne, Lausanne, Switzerland
20 Lawrence Livermore National Laboratory, Livermore, California, United States of America
21 Los Alamos National Laboratory, Los Alamos, New Mexico, United States of America
22 Institut de Physique Nucléaire de Lyon, IN2P3-CNRS/Université Claude Bernard, Villeurbanne, France
23 Centro de Investigaciones Energeticas, Medioambientales y Tecnologicas, CIEMAT, Madrid, Spain
24 Institute of Theoretical and Experimental Physics, ITEP, Moscow, Soviet Union
25 INFN-Sezione di Napoli and University of Naples, Italy
26 University of Nymegen and NIKHEF, Nymegen, The Netherlands
27 Oak Ridge National Laboratory, Oak Ridge, Tennessee, United States of America
28 California Institute of Technology, Pasadena, California, United States of America
29 Carnegie Mellon University, Pittsburgh, Pennsylvania, United States of America
30 Princeton University, Princeton, New Jersey, United States of America
31 INFN-Sezione di Roma and University of Roma, "La Sapienza", Italy
32 University of California, San Diego, California, United States of America
33 Union College, Schenectady, New York, United States of America
34 Shanghai Institute of Ceramics, SIC, Shanghai, China
35 Central Laboratory of Automation and Instrumentation, CLANP, Sofia, Bulgaria
36 University of Alabama, Tuscaloosa, Alabama, United States of America
37 Purdue University, West Lafayette, Indiana, United States of America
38 Paul Scherrer Institut, PSI, Würenlingen, Switzerland
39 Institut für Hochenergiephysik, Zeuthen, Federal Republic of Germany§
40 Eidgenössische Technische Hochschule, ETH Zürich Switzerland
41 University of Hamburg, Federal Republic of Germany
42 High Energy Physics Group, Taiwan, China
§ Supported by the German Bundesministerium für Forschung und Technologie

References

[1] H. Fritzsch, M. Gell-Mann and H. Leytwyler, *Phys. Lett.* **B 47** (1973) 365;
D.J. Gross and F. Wilczek, *Phys. Rev. Lett.* **30** (1973) 1343;
D.J. Gross and F. Wilczek, *Phys. Rev.* **8** (1973) 3633;
H.D. Politzer, *Phys. Rev. Lett.* **30** (1973) 1346.

[2] L3 Collaboration, B. Adeva et al., *Phys. Lett.* **B 248** (1990) 464.

[3] L3 Collaboration, B. Adeva et al., *Phys. Lett.* **B 257** (1991) 469.

[4] L3 Collaboration, B. Adeva et al., *Phys. Lett.* **B 248** (1990) 227.

[5] E. Laermann, K.H. Streng and P.M. Zerwas, *Z. Phys.* **C 3** (1980) 289
E. Laermann, K.H. Streng and P.M. Zerwas, to be publ. in *Z. Phys.* **C** (Erratum);
K. Koller et al., *Z. Phys.* **C 6** (1980) 131.

[6] N.M. Avram and D.H. Schiller, *Nucl. Phys.* **B 70** (1974) 272;
A.C. Hirschfeld and G. Kramer, *Nucl. Phys.* **B 74** (1974) 211;
G. Kramer, G. Schierholz and J. Willrodt, *Phys. Lett.* **B 79** (1978) 249
G. Kramer, G. Schierholz and J. Willrodt, *Phys. Lett.* **B 80** (1979) 433 (Erratum).

[7] P. Hoyer et al., *Nucl. Phys.* **B 161** (1979) 349.

[8] G. Kramer, G. Schierholz and J. Willrodt, *Z. Phys.* **C 4** (1980) 149.

[9] J.G. Körner, G.A. Schuler and F. Barreiro, *Phys. Lett.* **B 188** (1987) 272;
G.A. Schuler and J.G. Körner, *Nucl. Phys.* **B 325** (1989) 557.

[10] J. Ellis and I. Karliner, *Nucl. Phys.* **B 148** (1979) 141.

[11] TASSO Collaboration, R. Brandelik et al., *Phys. Lett.* **B 97** (1980) 453;
D. Lüke (TASSO Collaboration), Proceedings of the 21st International Conference on High Energy Physics, Paris (1982).

[12] L3 Collaboration, B. Adeva et al., *Nucl. Instrum. Methods* **A 289** (1990) 35.

[13] O. Adriani et al., CERN Preprint CERN-PPE/90-158.

[14] T. Sjöstrand, *Comput. Phys. Commun.* **39** (1986) 347;
T. Sjöstrand and M. Bengtsson, *Comput. Phys. Commun.* **43** (1987) 367.

[15] G. Marchesini and B. Webber, *Nucl. Phys.* **B 310** (1988) 461.

[16] L3 Collaboration, B. Adeva et al., *Phys. Lett.* **B 241** (1990) 416;
L3 Collaboration, B. Adeva et al., L3 Preprint # 27 (1991).

[17] GEANT Version 3.13, September, 1989.
See R. Brun et al., "GEANT 3", CERN DD/EE/84-1 (Revised), Sept. 1987;
To simulate hadronic interactions the program GHEISHA is used.
See H. Fesefeldt, RWTH Aachen Report PITHA 85/02 (1985).

[18] JADE Collaboration, W. Bartel et al., *Z. Phys.* **C 33** (1986) 23;
JADE Collaboration, S. Bethke et al., *Phys. Lett.* **B 213** (1988) 235.

[19] CELLO Collaboration, H.-J. Behrend et al., *Phys. Lett.* **B 110** (1982) 329.

[20] R.K. Ellis, D.A. Ross and E.A. Terrano, *Nucl. Phys.* **B 178** (1981) 421.

[21] PLUTO Collaboration, C. Berger et al., *Phys. Lett.* **B 97** (1980) 459.

[22] R. Clare (MARK J Collaboration), "QCD Properties of Jets", MIT Ph.D. Thesis (1982), unpublished.

[23] TASSO Collaboration, W. Braunschweig et al., *Z. Phys.* **C 47** (1990) 181.

Figure Captions

Figure 1 (a) Scaled parton energies and angles between jets for $e^+e^- \to q\bar{q}g$ for massless partons
(b) Angles θ and χ defining the orientation of a 3-jet event (from ref. [5])

Figure 2 Comparison of measured and predicted distributions with 3-jet events for $0.02 \leq y_{\rm cut} < 0.05$. The data are corrected for detector effects. The errors include statistical and systematic uncertainties. The horizontal bars indicate the bin width. The solid and dashed lines show the predictions for vector and scalar gluons, respectively. They include corrections for hadronization and photon radiation.
(a) scaled energy of the second jet, x_2
(b) scaled energy of third jet, x_3
(c) cosine of Ellis-Karliner angle, $\cos\lambda$
(d) cosine of angle of the first jet with respect to the beam direction, $\cos\theta$
(e) azimuthal angle of jet plane, χ
(f) cosine of polar angle of normal to jet plane with respect to the beam, $\cos\omega$

Figure 3 Comparison of measured and predicted distributions for 3-jet events as in figure 2, but for $y_{\rm cut} > 0.25$.

Figure 4 Comparison of measured and predicted mean values of the variables
(a) scaled energy of the second jet, x_2
(b) scaled energy of the third jet, x_3
(c) cosine of Ellis-Karliner angle, $\cos\lambda$
as a function of $y_{\rm cut}$. The errors (vertical bars) include statistical and systematic uncertainties. The horizontal bars indicate the bin width. The predictions for QCD and the scalar gluon model are shown as solid and dashed lines, respectively. They include corrections for hadronization and photon radiation.

Figure 5 Comparison of measured and predicted parameters
(a) α, see equation (4)
(b) β, see equation (5)
(c) γ, see equation (6)
as a function of $y_{\rm cut}$. The meaning of the errors is the same as for figure 4.

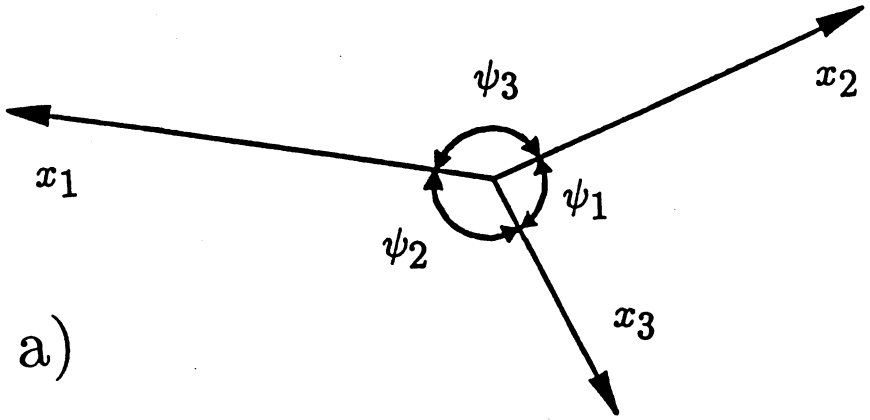
ψ_3
x_2
x_1
ψ_1
ψ_2
x_3
a)

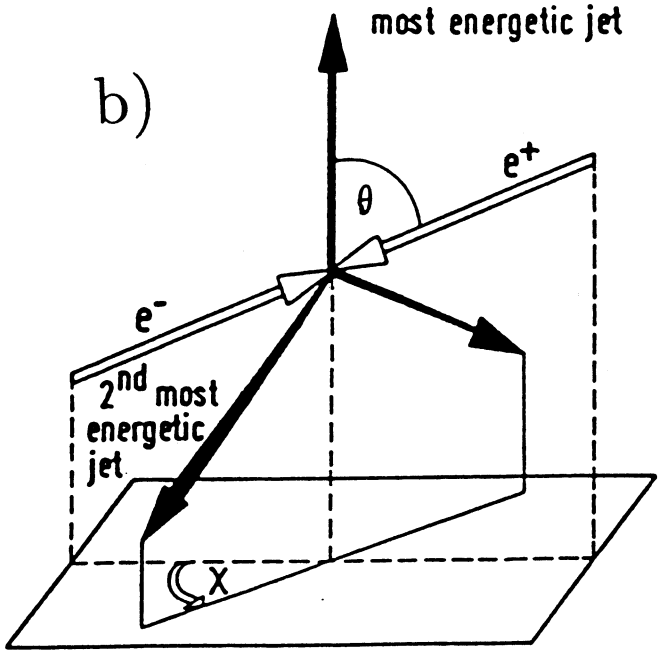
most energetic jet
b)
e^+
θ
e^-
2nd most energetic jet
χ

Figure 1

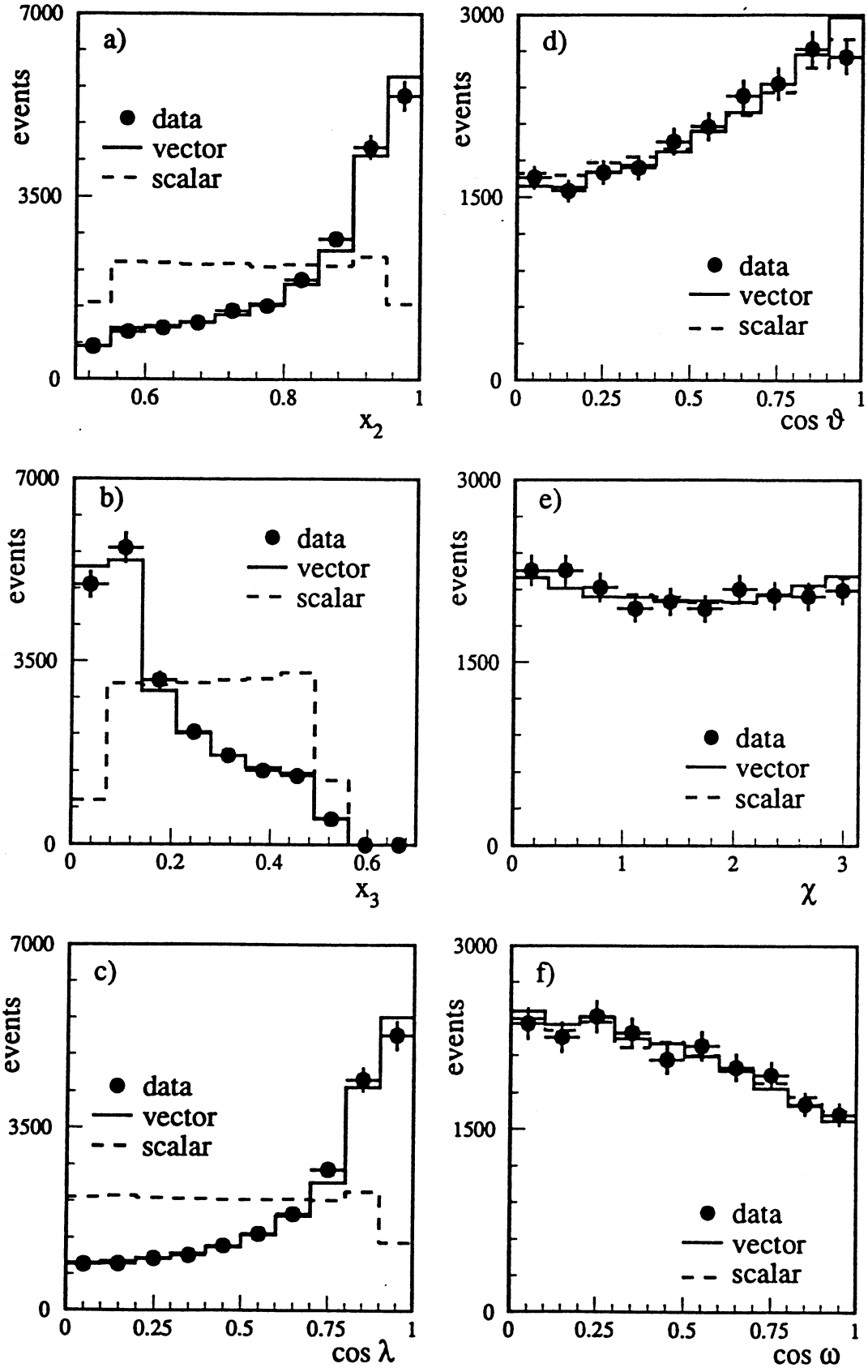
a)
data
vector
scalar
events
7000
3500
0
0.6
0.8
1
x_2
d)
3000
1500
0.25
0.5
0.75
cos ϑ
b)
0.2
0.4
x_3
e)
2
3
χ
c)
cos λ
f)
cos ω

Figure 2

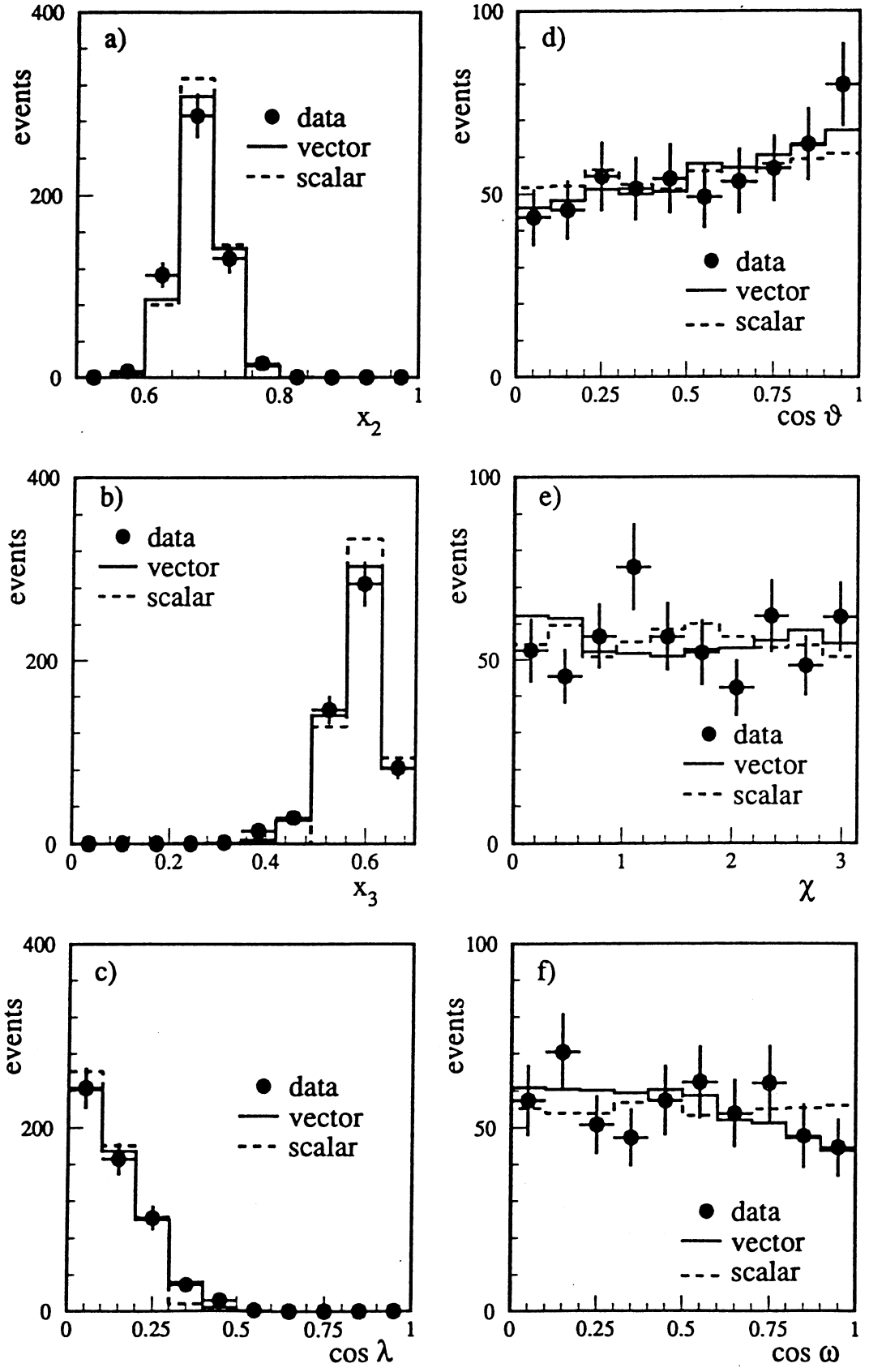
a)
events
data
vector
scalar
x_2
d)
events
data
vector
scalar
cos ϑ
b)
events
data
vector
scalar
x_3
e)
events
data
vector
scalar
χ
c)
events
data
vector
scalar
cos λ
f)
events
data
vector
scalar
cos ω

Figure 3

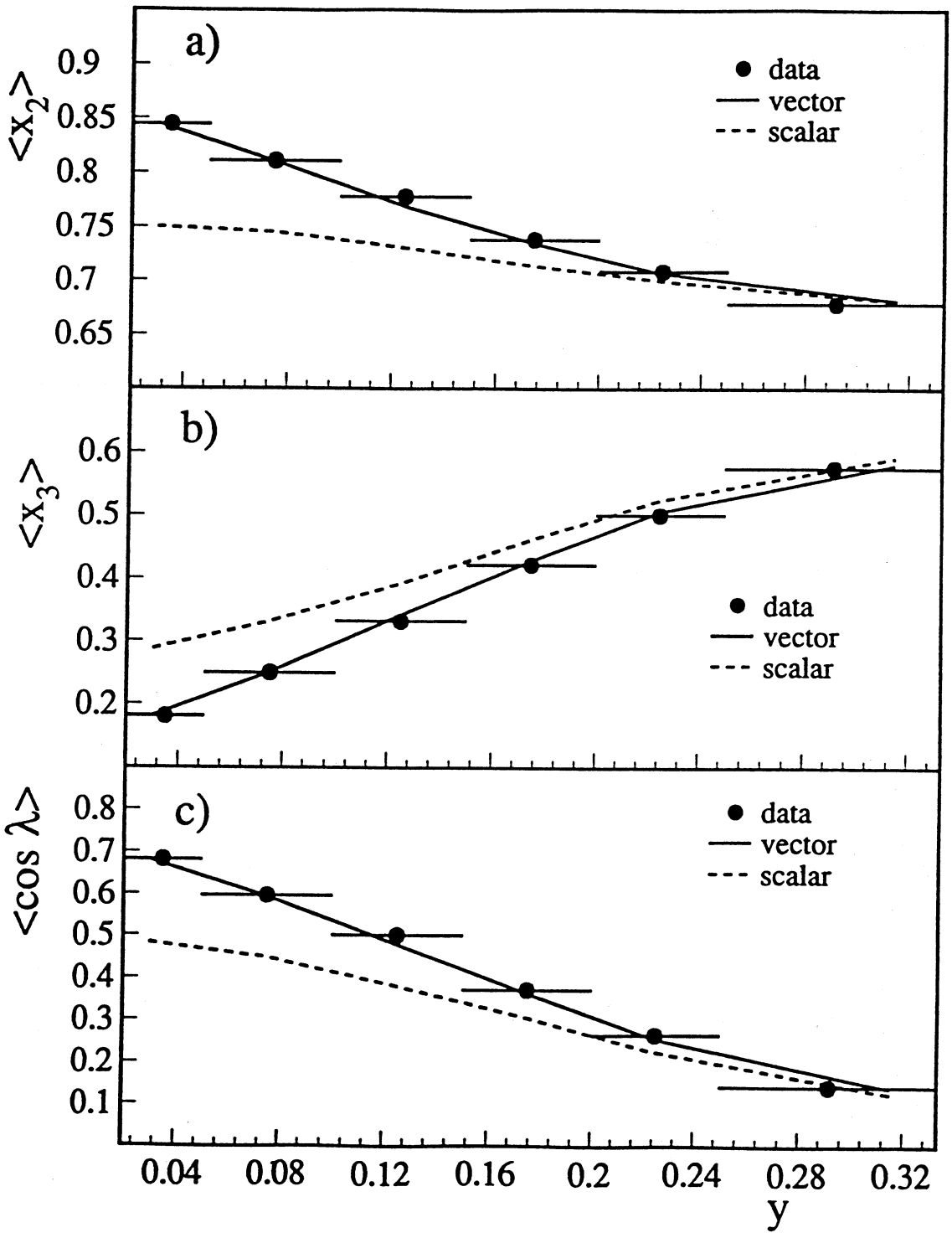
a)
b)
c)
data
vector
scalar
<x2>
<x3>
<cos λ>
0.9
0.85
0.8
0.75
0.7
0.65
0.6
0.5
0.4
0.3
0.2
0.1
0.04
0.08
0.12
0.16
0.2
0.24
0.28
0.32
y

Figure 4

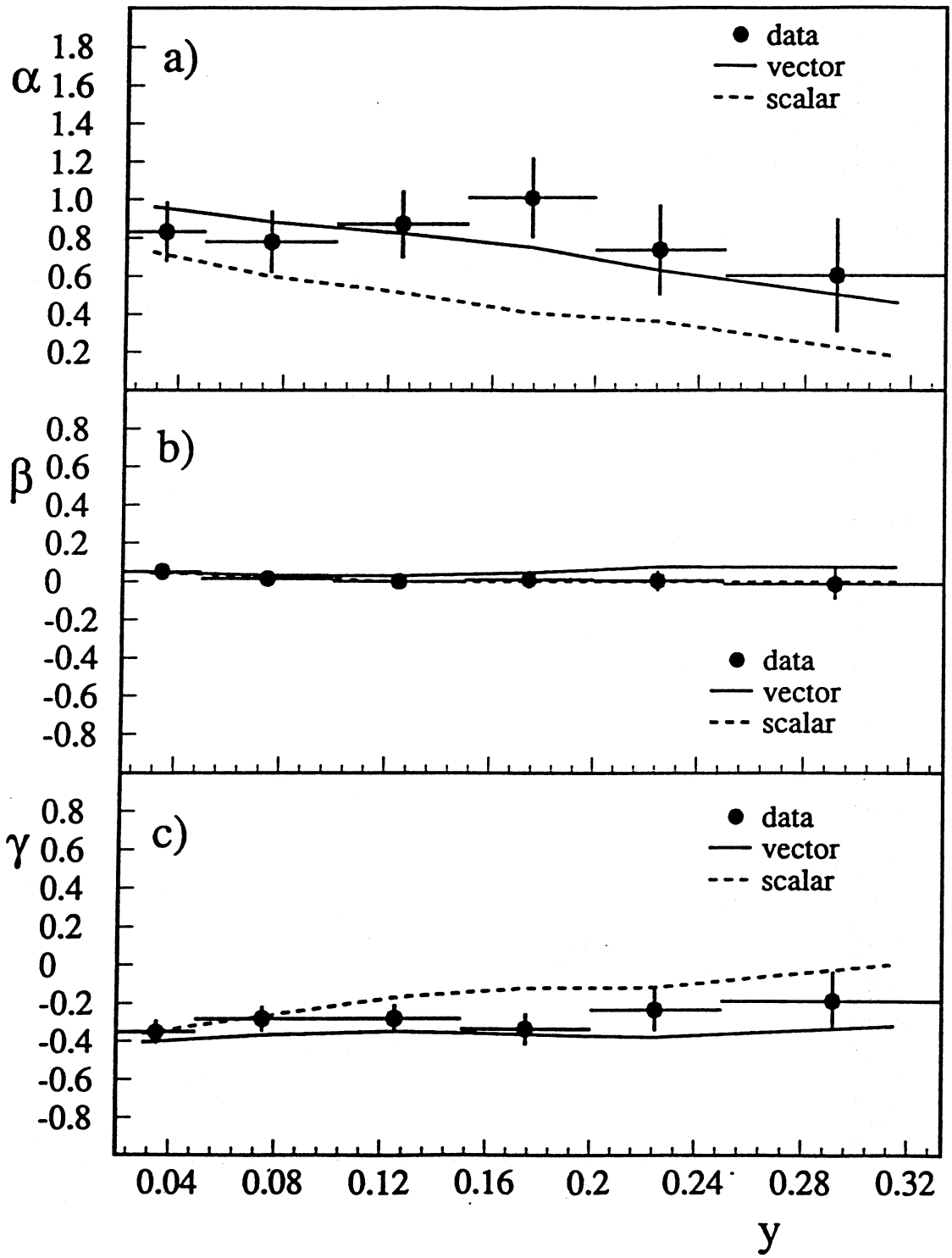

Figure 5

Imprimé au CERN. Prix : 0.80 Fr.